Study of the cubic to tetragonal transition in Mg_2TiO_4 and Zn_2TiO_4 spinels by ¹⁷O MAS NMR and Rietveld refinement of X-ray diffraction data

Roberta L. Millard, Ronald C. Peterson

Department of Geological Sciences, Queen's University, Kingston, Ontario K7L 3N6 Canada

Brian K. Hunter

Department of Chemistry, Queen's University, Kingston, Ontario K7L 3N6 Canada

Abstract

Cation ordering and structural changes in synthetic Mg_2TiO_4 and Zn_2TiO_4 spinels at temperatures across the polymorphic transition from the high-temperature cubic ($Fd3m$) to the low-temperature tetragonal ($P4_122$) structure are examined by ¹⁷O magic-angle spinning (MAS) NMR (9.4 T) and Rietveld structure refinement of powder X-ray diffraction data. The ¹⁷O NMR spectra of cubic Mg_2TiO_4 and Zn_2TiO_4 are similar, each showing one broad peak, positioned at 303 and 301 ppm, respectively. At the transition to the tetragonal phase, spectra of both Mg_2TiO_4 and Zn_2TiO_4 show significant narrowing because of the onset of long-range cation ordering in the tetragonal structure. The ¹⁷O NMR spectrum of tetragonal Zn_2TiO_4 shows two narrow peaks, at 301 and 273 ppm, corresponding to the two crystallographically distinct O sites in the tetragonally distorted spinel, showing that ¹⁷O chemical shift is sensitive to octahedral Zn-Ti substitution in Zn_2TiO_4. In contrast, the ¹⁷O NMR spectrum of tetragonal Mg_2TiO_4 shows only one peak, at 298 ppm. The structures of cubic and tetragonal Mg_2TiO_4 and Zn_2TiO_4 are compared. Tetragonal Zn_2TiO_4 exhibits greater distortion than Mg_2TiO_4 at the M1, O1, and O2 sites. These subtle structural differences do not explain differences in the ¹⁷O NMR spectra.

The ¹⁷O NMR spectra of the cubic Mg_2TiO_4 and Zn_2TiO_4 show no change with quench temperature above the transition to the cubic phase, suggesting that short-range ordering does not occur in cubic Mg_2TiO_4 and Zn_2TiO_4. A two-phase region is observed for both Mg_2TiO_4 and Zn_2TiO_4, below 664 and 561 °C, respectively, where the cubic and tetragonal phases are shown to be at equilibrium.

The ¹⁷O peak position of $MgTiO_3$ is observed at 398 ppm. This chemical-shift displacement of 100 ppm to high frequency of Mg_2TiO_4 is related to increased distortion in $MgTiO_3$.

Introduction

The spinel structure is a face-centered cubic arrangement of O anions with two types of cations, A and B, substituting into one-half of the available octahedral and one-eighth of the available tetrahedral sites, giving the general formula AB_2O_4. Cation ordering between tetrahedral and octahedral sites produces a range of disordered cation distributions bounded by two end-member ordered distributions, normal ($A[B_2]O_4$) and inverse ($B[AB]O_4$) (where [ ] denote octahedral site). For a detailed treatise on spinels, see, for example, Hill et al. (1979). In inverse spinels ($B[AB]O_4$), the two different types of cations occupying the octahedral sites are either ordered or disordered. Many spinels undergo distortion upon ordering at low temperatures (e.g., Preudomme and Tarte, 1980). This has been the subject of much structural modeling (Haas, 1965; Billet et al., 1967; Talanov, 1990). Among these spinels are Mg_2TiO_4 and Zn_2TiO_4.

Magnesiotitanate spinel (Mg_2TiO_4) is most closely ap- proached in nature as the mineral qandilite (Al-Hermezi, 1985), a Mg_2TiO_4-rich spinel occurring in the Mg_2TiO_4-Fe_2TiO_4-$MgFe_2O_4$-$FeFe_2O_4$ quadrilateral (Gittins et al., 1982). These spinels form part of an important group of spinels used as petrogenetic indicators of temperature and pressure accompanying geological processes (e.g., Sack and Ghiorso, 1991). The thermodynamic properties and structure of synthetic Mg_2TiO_4 have been studied by Wechsler and Navrotsky (1984) and Wechsler and Von Dreele (1989), respectively, and this spinel has been the subject of thermodynamic modeling (Hill and Sack, 1987; Sack and Ghiorso, 1991). Mg_2TiO_4 is an inverse spinel, having the structural formula $Mg[MgTi]O_4$. At high temperatures, the spinel is cubic ($Fd3m$). At temperatures below 660 °C (Wechsler and Navrotsky, 1984), the structure undergoes tetragonal distortion to $P4_122$ be- cause of long-range ordering of Mg^{2+} and Ti^{4+} cations on the octahedral sublattice. On the basis of calorimetric data, Wechsler and Navrotsky (1984) suggested that short-range ordering occurs above the transition to cubic in magne-

siotitanate spinel. Their data were insufficient to indicate how far above the transition the short-range ordering might persist, but they proposed two models, one that predicted ordering persisting to high temperature (1600 °C) and another that predicted the spinel would be disordered by 800 °C.

Zn_2TiO_4 undergoes tetragonal distortion to $P4_122$ at temperatures below 560 °C (Billet et al., 1967; Delamoye et al., 1967, 1970). Phase equilibria in this system have been studied by Dulin and Rase (1960), Bartram and Slepetys (1961), and others. Jacob and Alcock (1975) suggested from thermodynamic evidence that cubic Zn_2TiO_4 contains short-range ordering.

Short-range ordering in cubic spinels cannot be measured directly by diffraction methods because the space group ($Fd3m$) represents an average distribution of cations. However, locally, the distribution of cations varies. Because NMR is sensitive to the local environment around the nucleus of interest, ^{17}O MAS NMR has the potential to distinguish between these various local cation distributions around O and thus allows observation of short-range ordering in cubic spinels.

We used ^{17}O magic-angle spinning nuclear magnetic resonance spectroscopy (^{17}O MAS NMR), henceforward shortened to ^{17}O NMR, to study Mg_2TiO_4 and Zn_2TiO_4 spinels quenched from temperatures through the cubic to tetragonal phase transition and to examine the potential of ^{17}O NMR for measuring the short-range ordering thought to occur in these spinels. We refined the structures of both cubic and tetragonal Mg_2TiO_4 and Zn_2TiO_4 by Rietveld refinement of powder X-ray diffraction data to relate the ^{17}O NMR spectra of the titanate spinels to structural parameters such as site size and distortion and cation substitution.

THE MODEL

Assuming Mg_2TiO_4 and Zn_2TiO_4 to be completely inverse (Wechsler and Von Dreele, 1989), both the cubic and tetragonal titanate spinels ($B[TiB]O_4$) contain O atoms bonded to four cations: one B cation (B = Mg or Zn) in tetrahedral coordination and three cations (B, Ti, or both) in octahedral coordination. In the cubic spinel, O atoms are constrained by $Fd3m$ symmetry to be identical, giving one average O site and one average octahedral cation site, over which one B and one Ti are randomly distributed. A random cation distribution around the O site in the cubic spinel would result in four possible local environments around O, where the three octahedral cations would be 3Ti, 2Ti + B, Ti + 2B, and 3B in a ratio of 1:3:3:1. This suggests that the single crystallographically distinct O site in the cubic spinel could produce four peaks in the ^{17}O NMR spectrum.

The fully ordered tetragonal spinel has two unique O sites, both crystallographically (long range) and locally. The O1 and O2 sites have nearest-neighbor octahedral cation populations of Ti + 2B and 2Ti + B, respectively. We anticipate that the two cation environments around O in the tetragonal spinel would produce two peaks in

the ^{17}O NMR spectrum. In this case, the two local cation environments around O predicted for NMR are equivalent to the two crystallographically distinct O sites in the ordered tetragonal spinel.

EXPERIMENTAL METHODS

Synthesis

Cubic magnesiotitanate spinels were synthesized by sintering stoichiometric mixtures of previously dried (1000 °C), analytical-grade oxides for 18–36 h at about 1400 °C. Samples heated longer than 6 h were reground once. Cubic zinc titanate spinels were similarly prepared by sintering at about 1200 °C for 63–81 h with one regrinding. Tetragonally distorted spinels were prepared by heating the cubic samples at about 500 °C for at least 717 h for Mg_2TiO_4 and 264 h for Zn_2TiO_4. Details of syntheses and heating experiments for Mg_2TiO_4 and Zn_2TiO_4 are summarized in Tables 1 and 2, respectively.

The ^{17}O-enriched samples were prepared from ^{17}O-enriched TiO_2, which was prepared by the idealized reaction $TiCl_4 + 4H_2O = Ti(OH)_4 + 4HCl$, using 26.8% ^{17}O-enriched H_2O (MSD Isotopes, Quebec, Canada). The room temperature precipitate was a complex titanium oxychloride hydrate. TiO_2 (anatase) was prepared from the precipitate by drying under N_2 and heating at 500 °C for 1 h in air.

The ^{17}O-enriched oxide mixtures were sintered in Pt tubing under N_2 to prevent exchange of ^{17}O with ^{16}O in air. Tetragonally distorted spinels enriched in ^{17}O were heated in vacuum-sealed Pyrex tubing. Restriction of O in the system often resulted in some gray or blue coloration. Dark gray coloration was reduced to pale gray by heating the samples in air for 5–10 min. Sample coloration did not visibly affect NMR spectra.

Excess MgO and ZnO (1–3%) were found in most synthetic Mg_2TiO_4 and Zn_2TiO_4 samples, respectively. This excess is attributed to weighing errors, which resulted from ignoring the heavier mass of O from the 26.8% isotopically enriched $H_2{}^{17}O$ in the syntheses of TiO_2. Using the corrected mass for TiO_2 in later syntheses resulted in MgO-free samples in the case of Mg_2TiO_4 (RLM445 and RLM446) (see spectra Fig. 1a and 1b). However, after applying the corrected mass of O in Zn_2TiO_4 (RLM509 and RLM510), 1% ZnO remained. The amount of excess oxide remained constant throughout the heating experiments, as indicated by integration of NMR spectra.

Heating experiments

Mg_2TiO_4 samples were heated at temperatures between 1405 and 490 °C for various periods of time, as indicated in Table 1. Zn_2TiO_4 samples were heated at temperatures between 1210 and 490 °C, as indicated in Table 2. Most samples were contained in Pt tubing and heated in a vertical tube furnace (Deltech, Denver, Colorado). They were quenched in liquid N_2. A few of the samples (as indicated in the tables) were heated in muffle furnaces in vacuum-sealed Pyrex tubes. Temperature reversals were made at

TABLE 1. Thermal history of Mg_2TiO_4 spinels

Sample	Heating expts.		Structural state		Description	
	T (°C) (±2)	t (h)	Initial	Final	Color	Other phases
RLM445	1405	18	syn	C	w	none
RLM416	1399	6	C	C	w	MgO
RLM415	1003	113	C	C	w	MgO + G
RLM413*	800	330	C	C	w + gr	MgO
RLM422	702	3	T	C	gr	MgO
RLM430	664	36	T	C	w	MgO
RLM433	651	22	T	T + C	w	MgO
RLM447	651	99	C	C + T	w	MgO
RLM448	651	99	T	T + C	w	MgO
RLM432	641	22	T	T (+C)	w	MgO
RLM431	632	24	T	T (+C)	w	MgO
RLM426	606	26.5	T	T	w	MgO
RLM423*	500	837	C	T	gr	MgO
RLM446*	490	717	C	T	w	none

Note: C = cubic; T = tetragonal, with most abundant phase listed first; w = white; gr = gray; G = geikielite; parentheses indicate small amount of phase.
* Heated in a muffle furnace (error ±5 °C).

about 650 °C for Mg_2TiO_4 (Table 1) and 540 °C for Zn_2TiO_4 (Table 2). Note that near 1000 °C Mg_2TiO_4 partially decomposed into MgO and geikielite ($MgTiO_3$).

Nuclear magnetic resonance (NMR) spectroscopy

The ^{17}O MAS NMR spectra were acquired at 54.24 MHz as described previously (Millard et al., 1992). The spectra were acquired using a B_1 pulse width of 1.5 μs, a spectral width of 100 KHz with 2048 or 4096 data points, and a delay of 1 or 5 s between pulses. The solution (H_2O) $\pi/2$ pulse was 17 μs. Peak positions are reported relative to H_2O and were not corrected for field-dependent quadrupole effects. Peak positions and line widths were determined by fitting the spectra (Fourier transformed with no line broadening) with a Marquardt-Levenberg algorithm, using the program NMR-286 (SoftPulse Software, Guelph, Ontario) using Gaussian lines.

Extra phases occurring in the titanate spinel samples were readily identified by peak position. These were MgO (47–48 ppm), ZnO (−18 ppm), and, in one sample (RLM415), $MgTiO_3$ (398 ppm). The identity of the $MgTiO_3$ peak was confirmed by subsequent synthesis and

^{17}O NMR of $MgTiO_3$. Several spectra also contain a small peak at 377–378 ppm because of the Mg-bearing zirconia rotor.

Spin-lattice relaxation time constants (T_1) for both cubic and tetragonal Mg_2TiO_4 and Zn_2TiO_4 were measured by saturation-recovery experiments. Spin-relaxation data were fitted to a sum of two exponentials, allowing a best estimation of the longest relaxation component. The long T_1 values for cubic and tetragonal Zn_2TiO_4 were determined to be 18 and 27–30 s, respectively, and the long T_1 values for cubic and tetragonal Mg_2TiO_4 were determined to be 62 and 56 s, respectively.

X-ray methods

Preliminary work. The majority of samples were characterized after synthesis and heating experiments by the Guinier de Wolff film technique. Several samples contained some detectable ZnO but none contained TiO_2. MgO was not detectable on the films when occurring in very small amounts because of peak overlap with the spinel lines. $MgTiO_3$ was detected in one film (sample RLM415) because of spinel decomposition at 1000 °C.

TABLE 2. Thermal history of Zn_2TiO_4 spinels

Sample	Heating expts.		Structural state		Description	
	T (°C) (±2)	t (h)	Initial	Final	Color	Other phases
RLM509	1210	81	syn	C	w	ZnO
RLM511	601	60	C	C	w	ZnO
RLM512	581	72	C	C	w	ZnO
RLM516	561	281	C	C	w	ZnO
RLM526	555	402	T + C	C (+T)	w	ZnO
RLM521	540	371	C	C = T	w	ZnO
RLM522	540	371	T	C = T	w	ZnO
RLM524	529	315	C = T	T + C	w	ZnO
RLM510*	490	264	C	T (+C)	gr	ZnO
RLM527*	490	505	C + T	T (+C)	gr	ZnO

Note: C = cubic; T = tetragonal, with most abundant phase listed first; w = white; gr = gray; parentheses indicate small amount of phase; equal sign indicates approximately equivalent amounts.
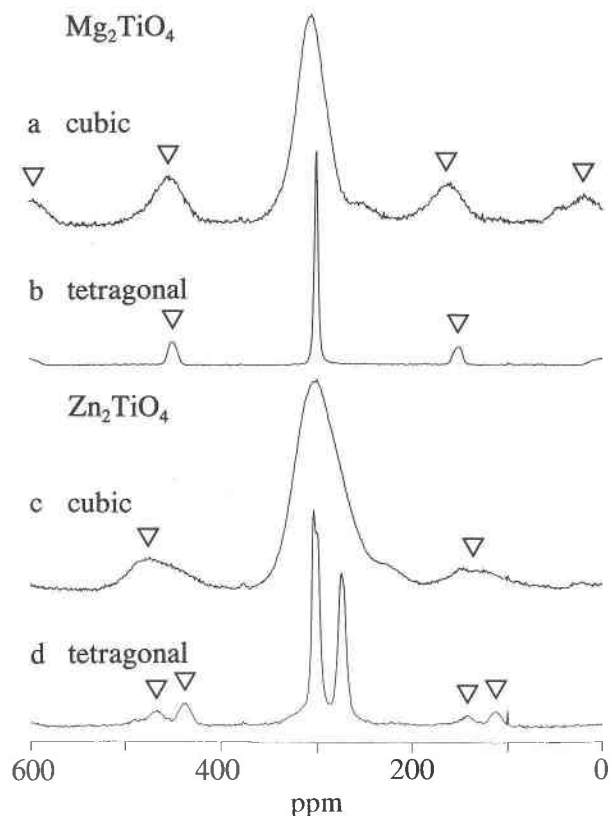* Heated in a muffle furnace (error ±5 °C).

Mg_2TiO_4

a cubic

b tetragonal

Zn_2TiO_4

c cubic

d tetragonal

600   400   200   0
ppm

Fig. 1.   The ^{17}O MAS NMR spectra (54.2 MHz) of synthetic cubic and tetragonal Mg_2TiO_4 and Zn_2TiO_4: (a) cubic Mg_2TiO_4 (RLM445), δ_{obs} = 303 ppm; (b) tetragonal Mg_2TiO_4 (RLM446), δ_{obs} = 298 ppm; (c) cubic Zn_2TiO_4 (RLM509), δ_{obs} = 301 ppm; (d) tetragonal Zn_2TiO_4 (RLM510), δ_{obs} = 301 and 273 ppm. Triangles denote spinning sidebands. The spike at 100 ppm is an artifact.

Data collection for Rietveld refinement. Powder X-ray diffraction data for Mg_2TiO_4 and Zn_2TiO_4 spinels were collected on a Rigaku D/MAX-1000 X-ray diffractometer (Danvers, Massachusetts) (40 kV, 40 Ma) with a θ-2θ geometry and a curved single-crystal graphite monochromator [(002); $2d$ = 6.708 Å], using $CuK\alpha$ radiation (λ = 1.54187 Å). Step-scan data were collected between 10 and 140° 2θ at 0.020 or 0.024° intervals with a count time of 4 s. Slit widths were as follows: divergence slit = scatter slit = 1 mm; receiving slit = 0.3 mm; and receiving slit for the monochromator = 0.45 mm. This gave maximum intensities of 4000–10000 total counts for Mg_2TiO_4 samples and 14000–22000 total counts for Zn_2TiO_4 samples. Data for one of the mixtures (RLM526) were collected at CSIRO, Melbourne, Australia, on a Phillips PW1710 diffractometer (Einhover, Holland) (40 kV, 40 Ma) with incident-beam Ge-monochromated $CuK\alpha_1$ radiation, to allow better phase resolution. Data were collected from 17 to 140° 2θ at 0.025° intervals with a count time of 17 s. Maximum intensity was 26000 total counts.

Rietveld refinement of powder X-ray data. The cubic spinels were refined with space group $Fd3m$ [origin ($\bar{3}m$)

at ⅛, ⅛, ⅛ from $\bar{4}3m$], with tetrahedral and octahedral cations occupying sites 8a and 16d, respectively, and O occupying site 32e. The tetragonal spinels were refined with space group $P4_122$, with tetrahedral cations occupying site 4c, octahedral M1 and M2 cations occupying sites 4a and 4b, respectively, and O1 and O2 occupying separate 8d sites. Initial cell and atomic parameters for cubic and tetragonal Mg_2TiO_4 were taken from Wechsler and Von Dreele (1989). Initial cell and atomic parameters for cubic Zn_2TiO_4 were taken from Bartram and Slepetys (1961). Initial atomic parameters for tetragonal Zn_2TiO_4 were assumed to be the same as for Mg_2TiO_4 (Wechsler and Von Dreele, 1989), whereas the initial cell parameters were from ICDD card 19-1483. All sites were assumed to be fully occupied. When the chemistry of Zn_2TiO_4 was allowed to vary, while also conserving charge balance ($2Zn^{2+} = Ti^{4+} + \square$), the spinels were found to be stoichiometric within error.

Data were refined using the whole pattern, least-squares refinement program DBWS-9006 (Wiles and Young, 1981). Ionic scattering curves were used for the refinement. Peak profiles were fitted using the pseudo-Voigt profile function, with Lorentzian character of peaks modeled using mixing parameter $\eta = N_a + N_b (2\theta)$. Peak profiles were calculated to either 5 or 8 FWHM to either side of peak center. Peaks were corrected for asymmetry for 2θ less than 39°. Peak widths (FWHM) were modeled using the function $H^2 = U \tan^2 \theta + V \tan \theta + W$. The cubic data were corrected for preferred orientation using the March-Dollase function and a preferred orientation vector [111]. No preferred orientation correction was made for the tetragonal spinels. Background was modeled using a four-parameter polynomial function with origin at 30° 2θ. The parameter turn-on sequence was as follows: scale factor, sample displacement (or rarely, zero), first background parameter, cell parameter(s), more background parameters, and then the profile parameters (in order W, U, V, N_a, asymmetry, N_b) together with crystal structural parameters. Crystal structural parameters were refined in the following order: atomic positions (u parameter in cubic spinels), isotropic temperature factors (B_{iso}), and cation occupancy (degree of inversion in the cubic case). Refinement of data collected with incident-beam-monochromated X-rays required use of the modified Thompson-Cox-Hastings pseudo-Voigt profile function. In this case N_a, N_b, and asymmetry are replaced by X, Y, and Z profile parameters. The relevant profile functions are $\Gamma_G^2 = U \tan^2 \theta + V \tan \theta + W + Z/\cos^2 \theta$ and $\Gamma_L = X \tan \theta + Y/\cos \theta$. The refined parameters from the final refinements of both cubic and tetragonal Mg_2TiO_4 and Zn_2TiO_4 spinels are given in Tables 3 and 4, respectively.

Rietveld refinement of mixtures. All Zn_2TiO_4 spinels contained ZnO as an extra phase. ZnO was refined in space group $P6_3mc$ with Zn and O at separate 2b sites, as in Sabine and Hogg (1969) and Kisi and Elcombe (1989). Initial cell parameters, positional parameter z, and B_{iso} were taken from Abrahams and Bernstein (1969). Cell parameters were refined, and z and B_{iso} were held constant. Profile and half-width parameters were constrained

TABLE 3. Final Rietveld refinements for cubic Mg_2TiO_4 and Zn_2TiO_4

	Mg_2TiO_4		Zn_2TiO_4		
	RLM445 1405 °C	RLM509 1210 °C	RLM526 555 °C	RLM510 490 °C
Profile	p-V	p-V	TCH p-V	p-V
Displacement	0.0294(3)	−0.0110(2)	−0.0420(2)	−0.0875(4)
Scale* cubic	0.309(2)	0.170(1)	0.175(1)	0.0244(4)
Scale* tetrag.	—	—	0.142(1)	0.663(2)
Scale* ZnO	—	0.364(7)	0.297(6)	0.320(4)
a_0	8.44183(3)	8.46948(2)	8.47056(3)	8.4608(1)
U	0.0096(5)	0.0081(4)	0.02(4)**	0.031(1)**
V	−0.0157(9)	−0.0124(7)	−0.0016(8)**	−0.011(2)**
W	0.0183(4)	0.0178(3)	0.02(4)**	0.0193(5)**
N_a	0.36(1)	0.30(1)	$X = 0.064(3)$**	0.21(1)**
N_b	0.0037(2)	0.0049(2)	$Y = -0.008(1)$**	0.0041(2)**
Asymmetry	1.03(4)	0.29(2)	$Z = -0.02(4)$**	0.21(1)**
Fraction Ti:				
T	0.036(5)	0.002(5)	0.0	0.0
M	0.482(5)	0.499(5)	0.5	0.5
u (O)	0.2616(1)	0.2606(2)	0.2599(2)	0.2604(9)
B_{iso} T	0.53(4)	0.21(2)	0.38(2)†	0.19(1)†
M	0.41(2)	0.31(2)	0.47(2)†	0.29(1)†
O	0.62(4)	0.92(4)	0.72(5)†	0.04(4)†
Pref.	0.967(3)	0.987(3)	N.D.	N.D.
R_{wp}	16.07	11.50	12.96	9.59
R_p	11.29	7.78	9.13	6.28
R_{exp}	9.61	7.74	8.59	7.44
χ^2	2.79	2.22	2.28	1.66
R_b(cubic)‡	3.39 (100)	3.36 (99)	2.87 (82)	3.17 (13)
R_b(tetrag)‡	—	—	8.93 (17)	2.63 (86)
R_b(ZnO)‡	—	20.53 (1)	20.48 (1)	12.31 (1)

Note: p-V = pseudo-Voigt profile function; TCH p-V = modified Thompson-Cox-Hastings pseudo-Voigt profile function; pref. = preferred orientation (vector [111]); R_{wp} = weighted pattern R-factor = 100 [Σ $w_i(y_i - y_{ci})^2/Σ w_i y_i^2$]$^{1/2}$, where $w_i = 1/y_i$, y_i = observed intensity at ith step, y_{ci} = calculated intensity at the ith step; R_p = pattern R-factor = 100 Σ|$y_i - y_{ci}$|/Σ|y_i|; R_{exp} = expected R-factor = 100 [(N − P + C)/Σ $w_i y_i^2$]$^{1/2}$, where N = no. observations, P = no. parameters, C = no. constraints; R_b = Bragg index = 100 Σ|"I_o" − I_c|/Σ"I_o", where "I_o" and I_c are the deduced observed and calculated intensities for the Bragg reflections; $\chi^2 = (R_{wp}/R_{exp})^2$. N.D. = not done.

  * Scale factors are × 10^3.

  ** Profile parameters were constrained to be equal for all phases.

  † Temperature factors were constrained to equal that of the equivalent site in tetragonal spinel.

  ‡ Percentage of phase is listed in parentheses after R_b. Phase percentages are calculated as $W_p = S_p(ZMV)_p/Σ S_i(ZMV)_i$, where S = scale factor, Z = no. of formula units per unit cell, M = mass of formula unit, V = volume of unit cell (cubic angstroms), from Hill (1993).

to be equal to those of the spinel. Refined cell parameters for ZnO were a_0 = 3.2501(3) and b_0 = 5.2053(5) Å. Samples contained about 1% ZnO, calculated as in Hill (1993) (Table 3).

For mixtures containing cubic and tetragonal Zn_2TiO_4, the profile and half-width parameters were constrained to be equal for both phases. Also, B_{iso} values for cations in similar sites in both cubic and tetragonal phases were constrained to be equal. For mixtures of both cubic and tetragonal Zn_2TiO_4, better refinements were obtained for small amounts of cubic phase than for small amounts of tetragonal phase because of the larger number of refinable parameters necessary in the tetragonal phase. We obtained a successful refinement of minor cubic Zn_2TiO_4 (13%) (RLM510, Table 3), whereas refinement of a small amount of tetragonal Zn_2TiO_4 (17%) (RLM526) was not satisfactory because of large uncertainties in atomic positional parameters.

RESULTS AND DISCUSSION

The ^{17}O MAS NMR of Mg_2TiO_4 and Zn_2TiO_4

The ^{17}O NMR spectra of both cubic and tetragonal Mg_2TiO_4 and Zn_2TiO_4 are shown in Figure 1. The spectra of cubic Mg_2TiO_4 and Zn_2TiO_4 are similar (Fig. 1a and 1c, respectively), each having one broad peak, centered at 301 (±4) and 303 (±4) ppm, respectively, with a shoulder to low frequency (260 and 250 ppm, respectively). The peak for cubic Zn_2TiO_4 is significantly broader than that for cubic Mg_2TiO_4 (2600 Hz vs. 2000 Hz), with a pronounced asymmetry. The low-frequency shoulder in the Zn_2TiO_4 spectrum also contains more intensity than that in the Mg_2TiO_4 spectrum (20–25% vs. 5–10%). The broad peaks in the spectra of the cubic spinels, with associated asymmetry and shoulders, suggest overlap of more than one O environment under this broad chemical-shift envelope. This chemical-shift dispersion is produced by a range of O environments related to disorder on the octahedral sublattice in these inverse spinels. The broad peaks in the ^{17}O NMR spectra probably include contributions from the four nearest-neighbor environments previously discussed, which have been broadened by the effect of next-nearest-neighbor substitution (and beyond). The increased broadening in the Zn_2TiO_4 spectrum suggests a larger chemical-shift dispersion between the O sites in this spinel than in Mg_2TiO_4 or greater second-order quadrupolar broadening.

The spectra of both tetragonal spinels (Fig. 1b and 1d)

TABLE 4. Final Rietveld refinements for tetragonal Mg_2TiO_4 and Zn_2TiO_4

	Mg_2TiO_4 RLM446	Zn_2TiO_4 RLM510
Profile	p-V	p-V
Displacement	−0.1043(5)	−0.0875(4)
Scale* tetrag	1.28(1)	0.663(2)
Scale* cubic	—	0.0244(6)
Scale* ZnO	—	0.320(4)
a_0	5.97705(6)	6.00689(4)
c_0	8.4161(1)	8.41547(8)
U	0.044(2)	0.031(1)**
V	−0.015(2)	−0.011(2)**
W	0.0237(6)	0.0193(5)**
N_a	0.24(1)	0.21(1)**
N_b	0.0016(3)	0.0041(2)**
Asymmetry	0.69(4)	0.21(1)**
Fraction Ti:		
T	0.0	0.0
M1	0.074(5)	0.087(5)
M2	0.926(5)	0.913(5)
Atomic coord.:		
T x	0.2518(4)	0.2529(2)
M1 y	0.2502(7)	0.2385(5)
M2 y	0.2391(4)	0.2470(6)
O1 x	−0.0264(6)	−0.0252(8)
y	0.7368(7)	0.7305(10)
z	0.2526(4)	0.2500(4)
O2 x	0.5188(7)	0.5131(8)
y	0.2610(8)	0.2638(11)
z	0.2329(4)	0.2307(4)
B_{iso} T	0.34(3)	0.19(1)†
M1	0.32(5)	0.29(1)†
M2	0.34(3)	fixed = M1
O1	0.29(7)	0.04(4)†
O2	0.31(7)	fixed = O1
R_{wp}	15.33	9.59
R_p	10.06	6.28
R_{exp}	9.71	7.44
χ^2	2.50	1.66
R_b(tetrag)‡	4.44 (100)	2.63 (86)
R_b(cubic)‡	—	3.17 (13)
R_b(ZnO)‡	—	12.31 (1)

Note: for explanation of abbreviated terms see Table 3.
* Scale factors are × 10³.
** Profile parameters for all phases have been constrained to be equal.
† Each temperature factor was constrained to equal that of the equivalent site in cubic phase.
‡ Percentages of phases are listed in parentheses beside R_b. For calculation of percent phases, see Table 3.

are significantly narrower than their cubic counterparts. Samples showing a broad peak in the NMR spectrum are confirmed to be cubic by X-ray methods, whereas samples showing narrow peaks are confirmed to be tetragonal by X-ray methods. Even the first appearance of narrow peaks in the NMR spectrum is accompanied by the appearance of weak tetragonal lines in the X-ray films. Therefore, we relate the narrow peaks in the ^{17}O NMR spectra to long-range 1:1 ordering on the octahedral sites. Long-range ordering results in a smaller chemical-shift dispersion in the tetragonal spinels compared with their cubic counterparts, producing at least a fivefold decrease in the line widths.

There is a striking difference between the ^{17}O NMR spectra of the tetragonal Mg_2TiO_4 and Zn_2TiO_4 spinels. The spectrum of tetragonal Mg_2TiO_4 shows one narrow peak (250 Hz) centered at 298 (± 2) ppm, whereas Zn_2TiO_4

exhibits two narrow peaks (500 Hz) centered at 301 (± 2) and 273 (± 2) ppm. The Zn_2TiO_4 peaks are asymmetric, and the high-frequency peak (301 ppm) exhibits second-order quadrupolar splitting. The larger line width, asymmetry, and peak splitting in tetragonal Zn_2TiO_4 relative to Mg_2TiO_4 suggest there is a larger quadrupole effect in Zn_2TiO_4. This is supported by double-rotation (DOR) spectra (Millard et al., unpublished data), which show a threefold decrease in the line width of the central transition over that by MAS, upon collapsing the second-order quadrupole effect.

We anticipated that the ^{17}O NMR spectra of the tetragonal spinels would be resolved into two peaks, representing the two different local (as well as crystallographically distinct) environments around O in the tetragonal spinel. Indeed, this was the case for tetragonal Zn_2TiO_4 but not for tetragonal Mg_2TiO_4. Instead, there is only one narrow peak in the ^{17}O NMR spectrum of Mg_2TiO_4 (Fig. 1b). Does this single peak represent the superposition of the resonances for the two O sites in the tetragonal spinel, or does it represent only one O site while the resonance for the second site is not visible? To distinguish between these possibilities, a quantitative experiment was performed, in which ^{17}O NMR spectra were collected from equimolar amounts of both tetragonal Mg_2TiO_4 and Zn_2TiO_4 under identical acquisition conditions and integrated using absolute intensities. The peak areas of the central peaks for both tetragonal Mg_2TiO_4 and Zn_2TiO_4 were within 5% of each other, showing that the single peak in the spectrum of tetragonal Mg_2TiO_4 is the result of two overlapping peaks. This implies that the O1 and O2 sites in Mg_2TiO_4 have very similar electronic environments. Another possibility, that the single peak results from rapid exchange between Mg and Ti at room temperature, is unlikely because of the sluggishness of the cubic to tetragonal transition (hundreds of hours) at 500 °C.

The effect of temperature on Mg_2TiO_4

The ^{17}O NMR spectra of Mg_2TiO_4 quenched from temperatures between 1405 and 664 °C were virtually identical to that in Figure 1a. The line width remained constant within experimental error, at 2000 (± 100) Hz. Figure 2 shows a series of ^{17}O NMR spectra from the same Mg_2TiO_4 sample quenched at various temperatures from 500 to 664 °C. The transition occurs below 664 °C. At 651 °C, both the cubic and tetragonal phases appear in the NMR spectrum (Fig. 2c) and X-ray pattern. To determine whether this mixture of phases was due to slow kinetics or a two-phase region, both a cubic sample and a tetragonal sample were heated in the same furnace at 651 °C. After 99 h, each sample contained a mixture of cubic and tetragonal phases, demonstrating the coexistence of two stable phases at 651 °C. This two-phase region extends over a range in temperature at least as low as 632 °C but not as low as 606 °C (see Table 1). Looking again at Figure 2b, a small amount of cubic material is
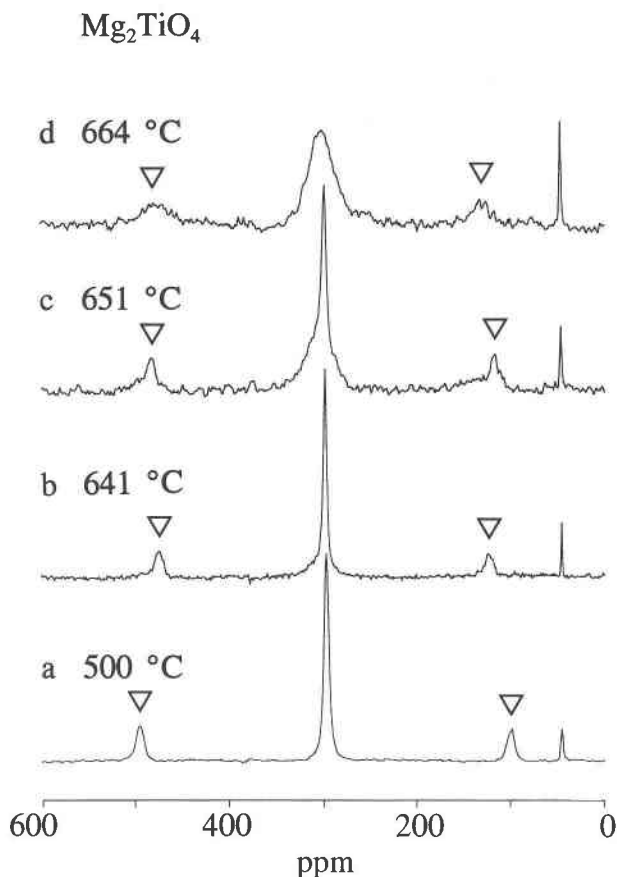
Mg_2TiO_4

Fig. 2. The ^{17}O MAS NMR spectra of Mg_2TiO_4 quenched from various temperatures between 500 and 664 °C: (a) tetragonal Mg_2TiO_4 (500 °C, 837 h); (b) the sample from a, heated to 641 °C (22 h); (c) the sample from b, heated to 651 °C (22 h); (d) the sample from c, heated to 664 °C (36 h). Note the mixture of two phases in spectra at intermediate temperatures (b and c). Triangles denote spinning sidebands. The narrow peak at 47 ppm is MgO.

Zn_2TiO_4

Fig. 3. The ^{17}O MAS NMR spectra of Zn_2TiO_4 quenched from various temperatures between 490 and 1210 °C: (a) cubic Zn_2TiO_4 (1210 °C, 81 h); (b) cubic sample heated at 561 °C (281 h); (c) tetragonal sample heated at 555 °C (402 h); (d) tetragonal sample heated at 540 °C (371 h); (e) tetragonal Zn_2TiO_4 (490 °C, 264 h). Note the mixture of two phases in spectra c, d, and e. Triangles denote spinning sidebands.

seen as a broad peak at the base of the narrow tetragonal peak after heating 22 h at 641 °C.

The effect of temperature on Zn_2TiO_4

Figure 3 shows a series of ^{17}O NMR spectra of Zn_2TiO_4 heated at various temperatures between 1210 and 490 °C. Note that the spectra in Figure 3c–3e contain both the cubic and tetragonal phases. This was verified by X-ray methods. To test for equilibrium in this two-phase region, both a cubic sample and a tetragonal sample of Zn_2TiO_4 were heated in the same furnace for various periods of time, at 540 °C. The resulting ^{17}O NMR spectra are shown in Figure 4. After 371 h the spectra are virtually identical, demonstrating that the two phases closely approach equilibrium. Fitting the spectra with Gaussian lines showed the cubic/tetragonal intensity ratios to be within 8% of each other. Figure 5 shows the observed, fitted, and component spectra for the sample used in Figure 4d. The existence of a two-phase region in Zn_2TiO_4
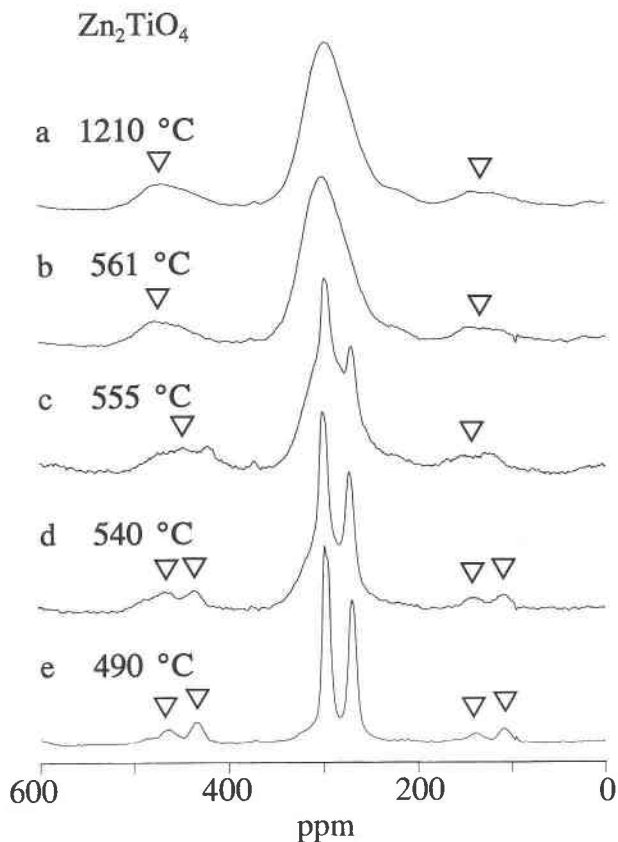
was demonstrated by Delamoye et al. (1970) between 552 and 560 (±2) °C. Our data show that this two-phase region extends over a wider temperature range [490–555 (±5) °C]. Even as low as 490 °C, the small broad peak at the base of the narrow doublet (Fig. 3e) suggests the presence of a minor cubic phase. This was verified by X-ray diffraction; Rietveld refinement indicated the presence of 13% cubic phase at 490 °C (Tables 3 and 4). This cubic phase persisted after 264 h at 490 °C, whereas Delamoye et al. (1970) reported complete transition from cubic to tetragonal phase in 2 h at 503 °C. To test the stability of the cubic phase, a subsequent sample was equilibrated for 505 h at 490 °C. This sample also contained the cubic phase, suggesting that the cubic spinel is stable as low as 490 °C.

The coexistence of two phases requires some chemical differentiation between the phases, but the differentiation is subtle. Rietveld refinement of these mixtures, allowing chemistry to vary while maintaining charge balance, showed both phases to be stoichiometric within error.

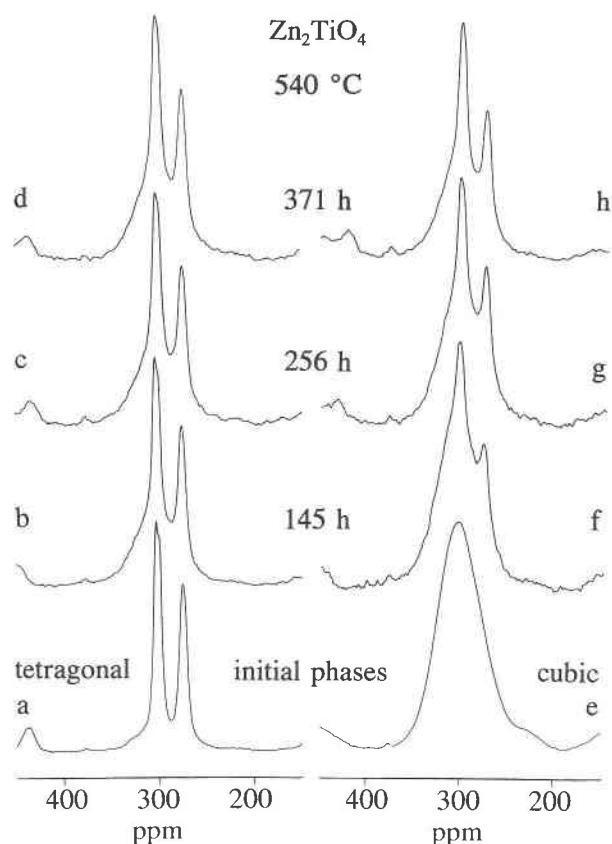Note that the fitted spectrum in Figure 5 also reveals

Fig. 4. The ^{17}O MAS NMR spectra of tetragonal and cubic Zn$_2$TiO$_4$ quenched from 540 °C after increasingly longer heating times, demonstrating equilibrium between tetragonal and cubic phases: (a–d) tetragonal sample heated for time periods indicated on the figure; (e–h) the identical heating series for the cubic sample. The spectra from d and h, respectively, give integrated intensities of 36 and 28% tetragonal phase.

Fig. 5. Observed, simulated, and difference ^{17}O MAS NMR spectra for the mixture of cubic and tetragonal Zn$_2$TiO$_4$ from Fig. 4d, showing the cubic and tetragonal components: (upper) observed spectrum; (middle) fitted spectrum, with component spectra represented by fine lines; (lower) difference spectrum.

that the intensity ratio of the tetragonal peaks is not 1:1 as expected but 60:40, where the high-frequency peak has higher intensity. This is not due to spin-lattice relaxation because saturation-recovery reveals similar relaxation behavior for both resonances (27 and 30 s for resonances at 301 and 273 ppm, respectively). This may relate to Zn-Ti disorder on the M1 and M2 sites in this spinel, but the relationship is unclear.

Lack of evidence for short-range ordering

Any short-range ordering occurring in cubic Mg$_2$TiO$_4$ or Zn$_2$TiO$_4$ should be observable in the ^{17}O NMR spectra as a gradual narrowing of the broad peak as the cations are distributed into specific sites, causing the site population around O to resemble that of the tetragonal spinel (for example, in Mg$_2$TiO$_4$, O1 and O2 have cation distributions of 2Mg + Ti and 2Ti + Mg, respectively). However, gradual line narrowing does not occur. Instead, there is an abrupt change from broad to narrow lines accompanying long-range ordering (Figs. 2 and 3) but no change in the spectra of cubic samples from temperatures above the transition temperature. Either complete dis-
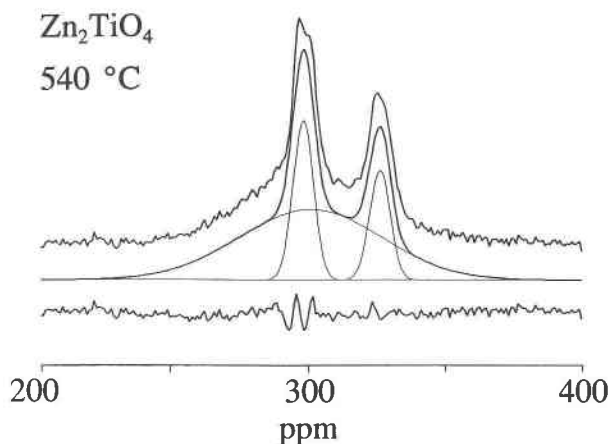
ordering occurs immediately at the transition to cubic and no short-range ordering exists or any short-range ordering in the cubic spinel remains unchanged to the highest temperature at which cation distributions can be quenched (thus the ^{17}O NMR spectrum is unchanged with increased temperature). However, because resonances for all cation environments around O occur in one broad chemical-shift envelope in the ^{17}O NMR spectrum, it is also possible that no net effect of short-range ordering can be observed in the spectra of cubic Mg$_2$TiO$_4$ and Zn$_2$TiO$_4$.

STRUCTURAL COMPARISON OF Zn$_2$TiO$_4$ AND Mg$_2$TiO$_4$

Cation ordering

The structures of cubic and tetragonal Mg$_2$TiO$_4$ have been reported by Wechsler and Von Dreele (1989). The structure of cubic Zn$_2$TiO$_4$ has been reported by Verwey and Heilmann (1947) and more recently by Bartram and Slepetys (1961). Tetragonal Zn$_2$TiO$_4$ is isomorphous with Mg$_2$TiO$_4$, having space group $P4_122$.

Tables 5 and 6 contain the cation-ordering information obtained from the present Rietveld refinement of cubic and tetragonal Mg$_2$TiO$_4$ and Zn$_2$TiO$_4$, respectively. The cubic Mg$_2$TiO$_4$ sample studied here was found to be 96.4(5)% inverse when quenched from 1405 °C. This sample is more disordered than the sample studied by Wechsler and Von Dreele (1989), who reported cubic Mg$_2$TiO$_4$ to be completely inverse. Cubic Zn$_2$TiO$_4$ was determined to be completely inverse at 1210 °C [99.8(5)%]. The tetragonal Mg$_2$TiO$_4$ sample studied here exhibited 7.4(5)% disorder between the M1 and M2 sites, in good agreement with that found by Wechsler and Von Dreele (1989) [8.5(4)%], with the M1 site primarily occupied by Mg^{2+}. Tetragonal Zn$_2$TiO$_4$ exhibited 8.7(5)% disorder at 490 °C, similar to that found for Mg$_2$TiO$_4$, with the M1 site occupied by Zn^{2+}.

For both tetragonal Mg$_2$TiO$_4$ and Zn$_2$TiO$_4$, the pres-

TABLE 5. Structural information from cubic Mg_2TiO_4 and Zn_2TiO_4

		Mg_2TiO_4	Zn_2TiO_4		
		RLM445 1405 °C (100%)	RLM509 1210 °C (99%)	RLM526 555 °C (82%)	RLM510 490 °C (13%)
Cell parameter	a_0	8.44183(3)	8.46948(2)	8.47056(3)	8.4608(1)
O	u	0.2616(1)	0.2606(2)	0.2599(2)	0.2604(9)
Ti fraction	T	0.036(5)	0.002(5)	0.0	0.0
	M	0.482(5)	0.499(5)	0.5	0.5
Bond lengths*	T-O	1.9973(8)	1.989(2)	1.979(2)	1.984(8)
	M-O	2.0173(8)	2.032(2)	2.037(2)	2.031(8)
	mean O-3M,T	2.0123(4)	2.021(1)	2.023(1)	2.019(4)

Note: number of bonds are T-O × 4; M-O × 6; cell parameters and bond lengths are in angstroms.
* Errors on mean bond lengths are calculated as $\sigma = (\Sigma\,\sigma_i^2)^{1/2}/n$.

ence of Ti in the tetrahedral site was tested by performing a series of block refinements, allowing Mg-Ti (or Zn-Ti) exchange between T and M2 sites and alternating with exchange between the M1 and M2 sites. Refinements of both Mg_2TiO_4 and Zn_2TiO_4 showed no Ti in the tetrahedral site within the error of the technique. This is consistent with <1% [4]Ti found in Mg_2TiO_4 by Wechsler and Von Dreele (1989).

Bond distances and polyhedral volume and distortion

Bond distances resulting from the Rietveld refinements of cubic and tetragonal Mg_2TiO_4 and Zn_2TiO_4 are listed in Tables 5 and 6, respectively. Examination of bond distances in the tetragonal spinels reveals that the shortest octahedral bonds are to Ti^{4+}, and some of these are shorter than the tetrahedral bonds to Mg^{2+} (or Zn^{2+}).

Mean bond distance, polyhedral volume, and polyhedral distortion for each site (including O) in both cubic and tetragonal Mg_2TiO_4 and Zn_2TiO_4 are listed in Table 7. Site distortion was measured by quadratic elongation (Robinson et al., 1971), which measures distortion from the symmetric configuration. Another measure of distortion, bond-length distortion (BLD) (Renner and Lehmann, 1986; Kunz et al., 1991) is also listed in Table 7 for comparison, but quadratic elongation is the distortion referred to in the text unless specified.

Examination of Tables 5, 6, and 7 shows the parallel nature of the structures of Mg_2TiO_4 and Zn_2TiO_4. In the cubic spinels, equivalent sites have similar size and distortion. Comparison of the cubic and tetragonal spinels reveals that the octahedral cation sites in both Mg_2TiO_4 and Zn_2TiO_4 follow the trend in size of M1 > M(cubic) > M2 and the trend in distortion of M1 > M(cubic) ≈ M2. The M1 site in Zn_2TiO_4 is significantly larger and more distorted than in Mg_2TiO_4. The greater distortion at the M1 site in Zn_2TiO_4 may be due to the ease of distortion of the d^{10} electron shell in Zn^{2+} (Cotton and Wilkinson, 1988). The size and distortion of the M2 site changes little between the structures of Mg_2TiO_4 and Zn_2TiO_4 because, in both structures, the M2 site is primarily occupied by Ti^{4+}.

It is interesting that quadratic elongation shows the M2 site, containing Ti^{4+}, to be less distorted from cubic symmetry than the M1 site containing Mg^{2+} and Zn^{2+}, where-

as BLD shows the M2 site to be more distorted than M1 (Table 7). Typically, sites containing Ti have high BLD values (Kunz et al., 1991).

Now consider the environment at the O sites. In all phases, the distortion from tetrahedral symmetry is high in the polyhedron of cations around O (Table 7) because this site is a trigonal pyramid (point symmetry $\bar{3}m$ in the cubic case). In Mg_2TiO_4 and Zn_2TiO_4, the O sites follow the trend in size of O2 > O1 ≈ O(cubic) and the trend in distortion of O1 > O2 > O(cubic), with O-site size and distortion being greater in Zn_2TiO_4.

STRUCTURAL AND CHEMICAL CONSIDERATIONS OF ^{17}O CHEMICAL SHIFT

Comparing tetragonal and cubic Mg_2TiO_4 and Zn_2TiO_4

If ^{17}O chemical shifts reflect site geometry, then we would expect the O1 and O2 sites to have similar geometry in tetragonal Mg_2TiO_4 (producing a single peak in ^{17}O NMR) but noticeably different geometries in tetragonal Zn_2TiO_4 (producing two peaks). However, struc-

TABLE 6. Structural information from tetragonal Mg_2TiO_4 and Zn_2TiO_4

		Mg_2TiO_4 RLM446	Zn_2TiO_4 RLM510
Cell parameters	a_0	5.97705(6)	6.00689(4)
	c_0	8.4161(1)	8.41547(8)
Ti fraction	T	0.0	0.0
	M1	0.074(5)	0.087(5)
	M2	0.926(5)	0.913(5)
Bond lengths*	T-O1	1.981(4)	1.977(5)
	T-O2	1.995(5)	1.980(6)
	M1-O1	2.090(3)	2.117(3)
	M1-O1	2.065(5)	2.065(6)
	M1-O2	2.088(5)	2.183(6)
	M2-O1	1.903(4)	1.922(6)
	M2-O2	2.039(5)	2.029(6)
	M2-O2	1.968(3)	1.946(3)
Mean	T-O	1.988(2)	1.979(3)
	M1-O	2.081(2)	2.122(2)
	M2-O	1.970(2)	1.966(2)
	O1-3M,T	2.010(2)	2.020(3)
	O2-3M,T	2.023(2)	2.035(3)

Note: all bonds are × 2; cell parameters and bond lengths are in angstroms.
* Errors on mean bond lengths are calculated as $\sigma = (\Sigma\,\sigma_i^2)^{1/2}/n$.

TABLE 7. Size and distortion of cation and O polyhedra in both cubic and tetragonal Mg_2TiO_4 and Zn_2TiO_4 spinels

Site	Mg_2TiO_4				Zn_2TiO_4			
	Cubic RLM445	Tetragonal RLM446			Cubic RLM509	Tetragonal RLM510		
Tetrahedral	Mg	Mg			Zn	Zn		
Mean T-O distance (Å)	1.997	1.988			1.989	1.979		
Polyhedral V (Å³)	4.09	4.03			4.04	3.97		
Quadratic elongation*	1.0000	1.0002			1.0000	1.0004		
Bond-length distortion** (%)	—	0.35			—	0.08		
Octahedral	M	M1		M2	M	M1		M2
	(Mg + Ti)	(Mg)		(Ti)	(Zn + Ti)	(Zn)		(Ti)
Mean M-O distance (Å)	2.017	2.081		1.970	2.032	2.122		1.966
Polyhedral V (Å³)	10.79	11.78		10.07	11.05	12.41		10.04
Quadratic elongation*	1.009	1.014		1.009	1.008	1.017		1.006
Bond-length distortion** (%)	—	0.51		2.34	—	1.93		2.15
O	O	O1		O2	O	O1		O2
Mean O-3M,T distance (Å)	2.012	2.010		2.023	2.021	2.020		2.035
Polyhedral V (Å³)	3.92	3.88		3.95	3.96	3.90		4.00
Quadratic elongation*	1.045	1.050		1.049	1.047	1.057		1.054
Bond-length distortion** (%)	0.37	3.37		2.03	0.80	3.50		3.66

* Quadratic elongation = $\lambda = (l_i/l_o)^2 = [(l_o + \Delta l)/l_o]^2 \approx 1 + 2\Delta l/l_o$. For an octahedral site, $\langle \lambda_{oct} \rangle = \Sigma_{i=1}^{6} (l_i/l_o)^2/6$, and similarly for the tetrahedral site, where l_o = length of line in unstrained state and l_i = length of line in strained state, from Robinson et al. (1971).
** Bond-length distortion (BLD) = $(100/n) \cdot \Sigma_{i=1}^{n} \{[|(M-O)_i - (M-O)_m|]/(M-O)_m\}$%, where m = mean bond length and n = number of bonds, from Kunz et al. (1991).

tural refinement shows only subtle differences in the structures of tetragonal Zn_2TiO_4 and Mg_2TiO_4. In Zn_2TiO_4, the O1 and O2 sites have a larger variation in both size and distortion than in Mg_2TiO_4. Comparing the O sites in Zn_2TiO_4, the O2 site is larger, and the O1 site is the more distorted from the symmetrical case. We do not know whether site size or distortion has a greater effect on the NMR chemical shift in the tetragonal spinels. Theoretical molecular orbital calculations of tetrahedral Si-O and Al-O bonding in silicates have shown a consistent correlation between $\angle$T-O-T and chemical shift (Tossell and Lazzeretti, 1987, 1988; Lindsay and Tossell, 1991), suggesting that distortion plays a more significant role. However, a strong empirical correlation between bond distance and ^{17}O chemical shift has been developed by Klemperer and coworkers (Filowitz et al., 1976; Klemperer, 1978; Che et al., 1985) for polyoxyanions.

The extent of a purely structural influence on chemical shift can be estimated in Mg_2TiO_4 by comparing the ^{17}O NMR spectra of cubic and tetragonal Mg_2TiO_4. The single peak in the spectrum of tetragonal Mg_2TiO_4 (containing the superposition of O1 and O2) is shifted 5 ppm to low frequency of the cubic peak centroid (303 to 298 ppm) on transition from the cubic to tetragonal phase. Because the two O sites do not behave independently (i.e., no effect of chemical substituents is obvious), this 5 ppm shift may be attributed to structural differences between the two phases. A similar difference in NMR peak position might be expected to occur between the polymorphs of isostructural Zn_2TiO_4 or a slightly higher difference because of the higher distortion in tetragonal Zn_2TiO_4, but this is unlikely to account for the entire 28 ppm difference between the ^{17}O peak positions of tetragonal Zn_2TiO_4 (273 and 301 ppm).

Now consider the chemical influences. Because the M2 site, containing Ti^{4+}, remains unchanged in size and dis-

tortion between Mg_2TiO_4 and Zn_2TiO_4 spinels, the observed peak positions must be caused by the other cation substituents. Why does replacement of Ti^{4+} with Zn^{2+} affect peak separation in the ^{17}O NMR spectrum of Zn_2TiO_4, whereas replacement of Ti^{4+} with Mg^{2+} has no net effect in ^{17}O NMR of Mg_2TiO_4? Some theoretical understanding of the substituent effect on chemical shift is being developed from molecular orbital theory for tetrahedral Si-O, Al-O, and P-O bonding (Tossell and Lazzeretti, 1987, 1988; Lindsay and Tossell, 1991; Tossell, 1993), but the problem remains that the environment around the O site has not yet been adequately modeled, including the proper number of coordinating cations (Tossell, 1993). In the absence of theoretical correlation between structure, chemistry, and chemical shift we consider empirical correlations.

The ^{17}O NMR resonances for Mg_2TiO_4 and Zn_2TiO_4 are observed in the chemical-shift region consistent with $^{[4]}O$ surrounded by Ti (O-4Ti; 250–450 ppm) (Day et al., 1992; Bastow et al., 1993). This is shifted to higher frequency than $^{[4]}O$ in $MgAl_2O_4$ spinel (O-Mg,3Al; 66 ppm) (Millard et al., 1992). The higher-frequency chemical shifts in the ^{17}O NMR spectra of the titanate spinels (303 ppm in Mg_2TiO_4 as compared to 66 ppm in $MgAl_2O_4$) are probably governed by paramagnetic deshielding from Ti^{4+} because of its highly oxidized state (Jameson and Mason, 1987).

Displacement of ^{17}O NMR chemical shift to low frequency on substitution of Zn^{2+} for Mg^{2+} has been observed previously in cubic $MgAl_2O_4$ and $ZnAl_2O_4$ spinels. Millard (1990) measured peak positions of 66 and 50 ppm for O in the ^{17}O NMR spectra of $MgAl_2O_4$ and $ZnAl_2O_4$, respectively, which is a 16 ppm shift to low frequency on replacement of Mg^{2+} with Zn^{2+} in the spinel structure of cubic aluminate spinels. The 25 ppm peak shift to low frequency (for one of the O sites) on replace-

ment of Mg^{2+} with Zn^{2+} in the tetragonal titanate spinels is consistent with this observation, showing that this substitution has a shielding effect on ^{17}O chemical shifts. This may be related to the unique orbital interaction between Zn^{2+} and O. Grimes et al. (1989) showed by structure-preference energy calculations on spinels that Zn^{2+}, unlike other 3d transition metals, destabilizes the O 2p orbitals.

On the basis of the empirical relationship noted above between Zn^{2+} and chemical shift, the O site with more Zn^{2+} substitution would probably be displaced to lower frequency. Recalling that the coordination around the O sites is O1-(3Zn,Ti) and O2-(2Zn,2Ti), we tentatively assign the low-frequency peak (273 ppm) in the spectrum of tetragonal Zn_2TiO_4 to O in the O1 site and the high-frequency peak (301 ppm) to O in the O2 site.

Comparing Mg_2TiO_4 and $MgTiO_3$

The ^{17}O NMR spectrum of geikielite ($MgTiO_3$) contains a single narrow peak (300 Hz) at 398 (±2) ppm. This peak is displaced 100 ppm to high frequency compared with that of tetragonal Mg_2TiO_4 (298 ppm). $MgTiO_3$ and Mg_2TiO_4 have similar chemical substituents, so the large ^{17}O chemical-shift displacement must be structurally controlled. Examination of the structures shows the chemical environment around the single O site in $MgTiO_3$ to be comparable to the O2 site in Mg_2TiO_4. Each O is bonded to two Mg and two Ti cations. We calculated the polyhedral volume and distortion for the O site in geikielite (O_g) using the data of Wechsler and Von Dreele (1989). Volume at O_g is 3.60 $Å^3$, mean O_g-M distance is 2.043 Å, quadratic elongation is 1.143, and BLD is 4.30%. The O polyhedron in $MgTiO_3$ is extremely distorted; the quadratic elongation at the O_g site is about three times that at the O2 site in Mg_2TiO_4, suggesting that site distortion plays a major role in determining these ^{17}O chemical shifts. The single Ti site in $MgTiO_3$ is also highly distorted, with three particularly short O-Ti bonds (1.867 Å), which are shorter than any bonds in Mg_2TiO_4. The BLD calculated for the Ti site in $MgTiO_3$ is 5.6% (vs. 2.9% at the Mg site). This is on the order of that found by Kunz et al. (1991) for octahedral sites with off-center Ti in neptunite, implying similar off-center behavior of Ti^{4+} in $MgTiO_3$. This suggests that the behavior of Ti in minerals, resulting in significant site distortion, can greatly affect ^{17}O chemical shift.

REFERENCES CITED

Abrahams, S.C., and Bernstein, J.L. (1969) Remeasurement of the structure of hexagonal ZnO. Acta Crystallographica, B25, 1233–1236.

Al-Hermezi, H.M. (1985) Qandilite, a new spinel end-member, Mg_2TiO_4, from the Qala-Dizeh region, NE Iraq. Mineralogical Magazine, 49, 739–744.

Bartram, S.F., and Slepetys, R.A. (1961) Compound formation and crystal structure in the system ZnO-TiO_2. Journal of the American Ceramic Society, 44, 493–499.

Bastow, T.J., Moodie, A.F., Smith, M.E., and Whitfield, H.J. (1993) Characterization of titania gels by ^{17}O nuclear magnetic resonance and electron diffraction. Journal of Materials Chemistry, 3, 697–702.

Billet, Y., Morgenstern-Badarau, I., and Michel, A. (1967) Contribution à l'étude des surstructures spinelles: Cas de l'ordre 1:1 en site B. Bulletin de la Société français de Minéralogie et de Cristallographie, XC, 8–19.

Che, T.M., Day, V.W., Francesconi, L.C., Fredrich, M.F., Klemperer, W.G., and Shum, W. (1985). Synthesis and structure of the $[(\eta^5\text{-}C_5H_5)Ti(Mo_5O_{18})]^{3-}$ and $[(\eta^5\text{-}C_5H_5)Ti(W_5O_{18})]^{3-}$ anions. Inorganic Chemistry, 24, 4055–4062.

Cotton, F.A., and Wilkinson, G. (1988) Advanced inorganic chemistry: A comprehensive text (5th edition), 1455 p. Wiley, New York.

Day, V.W., Eberspacher, T.A., Klemperer, W.G., Park, C.W., and Rosenberg, F.S. (1992) Oxygen-17 nuclear magnetic resonance spectroscopic study of titania sol-gel polymerization. In L.L. Hench and J.K. West, Eds., Chemical processing of advanced materials, p. 257–265. Wiley, New York.

Delamoye, P., Billet, Y., Morgenstern-Badarau, I., and Michel, A. (1967) Influence des écarts à la stœchiométrie sur la transformation ordre-désordre de l'orthotitanate de zinc. Bulletin de la Société français de Minéralogie et de Cristallographie, XC, 585–591.

Delamoye, P., Billet, Y., and Michel, A. (1970) Étude du phénomène ordre-désordre dans les solutions solides de l'orthotitanate de zinc. Annales de Chimie, 5, 327–334.

Dulin, F.H., and Rase, D.E. (1960) Phase equilibria in the system ZnO-TiO_2. Journal of the American Ceramic Society, 43, 125–131.

Filowitz, M., Klemperer, W.G., Messerle, L., and Shum, W. (1976) An ^{17}O nuclear magnetic resonance chemical shift scale for polyoxomolybdenates. Journal of the American Chemical Society, 98, 2345–2346.

Gittins, J., Fawcett, J.J. and Rucklidge, J.C. (1982) An occurrence of the spinel end-member Mg_2TiO_4 and related spinel solid solutions. Mineralogical Magazine, 45, 135–137.

Grimes, R.W., Anderson, A.B., and Heuer, A.H. (1989) Predictions of cation distributions in AB_2O_4 spinels from normalized ion energies. Journal of the American Chemical Society, 111, 1–7.

Haas, C. (1965) Phase transitions in crystals with the spinel structure. Journal of Physics and Chemistry of Solids, 26, 1225–1232.

Hill, R.J. (1993) Data collection strategies: Fitting the experiment to the need. In R.A. Young, Ed., The Rietveld method, p. 61–101. Oxford University Press, New York.

Hill, R.J., Craig, J.R., and Gibbs, G.V. (1979) Systematics of the spinel structure type. Physics and Chemistry of Minerals, 4, 317–339.

Hill, R.L., and Sack, R.O. (1987) Thermodynamic properties of Fe-Mg titaniferous magnetite spinels. Canadian Mineralogist, 25, 443–464.

Jacob, K.T., and Alcock, C.B. (1975) Evidence of residual entropy in the cubic spinel Zn_2TiO_4. High Temperatures–High Pressures, 7, 433–439.

Jameson, C.J., and Mason, J. (1987) The chemical shift. In J. Mason, Ed., Multinuclear NMR, p. 51–88. Plenum, New York.

Kisi, E.H., and Elcombe, M.M. (1989) μ parameters for the wurtzite structure of ZnS and ZnO using powder neutron diffraction. Acta Crystallographica, C45, 1867–1870.

Klemperer, W.G. (1978) ^{17}O-NMR spectroscopy as a structural probe. Angewandte Chemie International Edition, 17, 246–254.

Kunz, M., Armbruster, T., Lager, G.A., Schultz, A.J., Goyette, R.J., Lottermoser, W., and Amthauer, G. (1991) Fe, Ti ordering and octahedral distortions in acentric neptunite: Temperature dependent X-ray and neutron structure refinements and Mössbauer spectroscopy. Physics and Chemistry of Minerals, 18, 199–213.

Lindsay, C.G., and Tossell, J.A. (1991) Ab initio calculations of ^{17}O and

^nT NMR parameters (^nT = ^{31}P, ^{29}Si) in H_3TOTH_3 dimers and T_3O_9 trimeric rings. Physics and Chemistry of Minerals, 18, 191–198.

Millard, R.L. (1990) The temperature dependence of cation disorder in $MgAl_2O_4$ and cation disorder in $ZnAl_2O_4$ by aluminium-27 and oxygen-17 magic-angle spinning nuclear magnetic resonance spectroscopy. M.Sc. thesis, Queen's University, Kingston, Ontario, Canada.

Millard, R.L., Peterson, R.C., and Hunter, B.K. (1992) Temperature dependence of cation disorder in $MgAl_2O_4$ spinel using ^{27}Al and ^{17}O magic-angle spinning NMR. American Mineralogist, 77, 44–52.

Preudomme, J., and Tarte, P. (1980) Studies of spinels: VII. Order-disorder transition in the inverse germanate spinels $Zn_{2-x}(Co,Ni)_xGeO_4$ ($x \approx 1$). Journal of Solid State Chemistry, 35, 272–277.

Renner, B., and Lehmann, G. (1986) Correlation of angular and bond length distortions in TO_4 units in crystals. Zeitschrift für Kristallographie, 175, 43–59.

Robinson, K., Gibbs, G.V., and Ribbe, P.H. (1971) Quadratic elongation: A quantitative measure of distortion in coordination polyhedra. Science, 172, 567–570.

Sabine, T.M., and Hogg, S. (1969) The wurtzite z parameter for beryllium oxide and zinc oxide. Acta Crystallographica, B25, 2254–2256.

Sack, R.O., and Ghiorso, M.S. (1991) An internally consistent model for the thermodynamic properties of Fe-Mg-titanomagnetite-aluminate spinels. Contributions to Mineralogy and Petrology, 106, 474–505.

Talanov, V.M. (1990) Structural modelling of low-symmetry phases of spinels. Physica Status Solidi, B162, 61–73.

Tossell, J.A. (1993) A theoretical study of the molecular basis of the Al avoidance rule and of the spectral characteristics of Al-O-Al linkages. American Mineralogist, 78, 911–920.

Tossell, J.A., and Lazzeretti, P. (1987) Ab initio calculations of oxygen nuclear quadrupole coupling constants and oxygen and silicon NMR shielding constants in molecules containing Si-O bonds. Chemical Physics, 112, 205–212.

——— (1988) Calculation of NMR parameters for bridging oxygens in H_3T-O-$T'H_3$ linkages (T, T' = Al, Si, P), for oxygen in SiH_3O^-, SiH_3OH and SiH_3OMg^+ and for bridging fluorine in $H_3SiFSiH_3^+$. Physics and Chemistry of Minerals, 15, 564–569.

Verwey, E.J.W., and Heilmann, E.L. (1947) Physical properties and cation arrangement of oxides with spinel structures. Journal of Chemical Physics, 15, 174–180.

Wechsler, B.A., and Navrotsky, A. (1984) Thermodynamics and structural chemistry of compounds in the system MgO-TiO_2. Journal of Solid State Chemistry, 55, 165–180.

Wechsler, B.A., and Von Dreele, R.B. (1989) Structure refinements of Mg_2TiO_4, $MgTiO_3$, and $MgTi_2O_5$ by time-of-flight neutron powder diffraction. Acta Crystallographica, B45, 542–549.

Wiles, D.B., and Young, R.A. (1981) A new computer program for Rietveld analysis of X-ray powder diffraction patterns. Journal of Applied Crystallography, 14, 149–151.